



Synthesis and structure of 4-[(*E*)-(7-methoxy-1,3-benzodioxol-5-yl)methylidene]amino}-1,5-dimethyl-2-phenyl-2,3-dihydro-1*H*-pyrazol-3-one

Charmaine Arderne,^{a*} Marthe Carine Djuide Fotsing^b and Derek Tantoh Ndinteh^b

Received 29 December 2020

Accepted 22 January 2021

Edited by W. T. A. Harrison, University of Aberdeen, Scotland

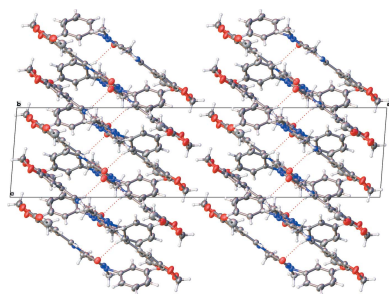
Keywords: crystal structure; Schiff bases; 4-aminoantipyrene; 4-aminophenazone.**CCDC reference:** 2058001**Supporting information:** this article has supporting information at journals.iucr.org/e

^aDepartment of Chemical Sciences, Research Centre for Synthesis and Catalysis, University of Johannesburg, PO Box 524, Auckland Park, Johannesburg, 2006, South Africa, and ^bDepartment of Chemical Sciences, University of Johannesburg, PO Box 17011, Doornfontein, Johannesburg, 2028, South Africa. *Correspondence e-mail: carderne@uj.ac.za

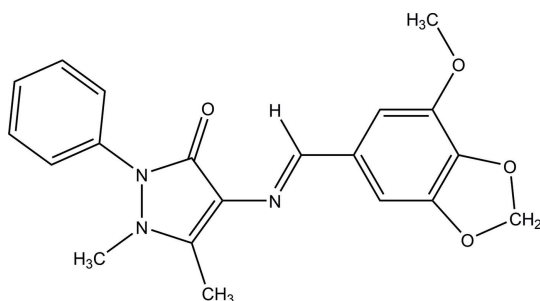
In the title compound, C₂₀H₁₉N₃O₄, the dihedral angles between the central pyrazole ring and the pendant phenyl and substituted benzene rings are 50.95 (8) and 3.25 (12)°, respectively, and an intramolecular C—H···O link generates an *S*(6) ring. The benzodioxolyl ring adopts a shallow envelope conformation with the methylene C atom as the flap. In the crystal, the molecules are linked by non-classical C—H···O interactions, which generate a three-dimensional network. Solvent-accessible voids run down the *c*-axis direction and the residual electron density in these voids was modelled during the refinement process using the *SQUEEZE* algorithm [Spek (2015). *Acta Cryst. C* **71**, 9–18] within the structural checking program *PLATON*.

1. Chemical context

Compounds such as 4-aminoantipyrene (4-amino-1,5-dimethyl-2-phenylpyrazole) and its Schiff base analogues are chemically attractive because of the various biological properties they possess, their synthetic flexibility and their selectivity and sensitivity towards metal ions (Keskiöglü *et al.*, 2008). Pyrazol-3-one Schiff bases can be obtained from the condensation of 4-aminophenazone or 4-aminoantipyrene (4-AAP) and the corresponding carbonyl compound (Sakthivel *et al.*, 2020). Schiff bases can find applications in analytical chemistry, material sciences and in various biological fields. In analytical chemistry, Schiff bases obtained from 4-AAP and 2-hydroxy-1,2-diphenylethanone have been used as a colorimetric sensor for Fe^{III} and as a fluorescent sensor for Al^{III} (Soufeena & Aravindakshan, 2019). Some other 4-aminophenazone analogues have been applied in the separation and determination of pentachlorophenol in treated softwoods and preservative solutions (Williams, 1971). In material sciences, the corrosion inhibition tendency of 4-AAP and its derivatives has also been discussed (Junaedi *et al.*, 2013). Other derivatives have also been used to improve solar cell efficiency (Ismail *et al.*, 2020). Various 4-AAP derivatives have several biological applications and 4-AAP Schiff bases from the condensation with *para*-methoxycinnamaldehyde display antimicrobial activity against a large spectrum of microorganisms (Obasi *et al.*, 2016). Still more 4-AAP derivatives show DNA binding and cleavage activity has also been reported (Rosenberg *et al.*, 1969). Several other biological applications include antioxidant, anti-inflammatory (Deng *et al.*, 2019), analgesic and antipyretic (Murtaza *et al.*, 2017)



among others. Platinum(II) complexes of Schiff bases have been reported as potential anti-cancer agents. Some of these complexes have a better toxicity than that of Cisplatin (Li *et al.*, 2013).



As part of our studies in this area, the title compound, $C_{20}H_{19}N_3O_4$, was obtained from 4-AAP and myristicin aldehyde and its crystal structure determined.

2. Structural commentary

The title compound (**I**) crystallizes in the monoclinic centrosymmetric space group $C2/c$, and the asymmetric unit consists of one non-planar independent molecule. The phenyl ring (C15–C20) is twisted away from the plane of the pyrazole ring moiety (N2/N3/C10–C12) by $50.95(8)^\circ$, most likely because of steric hindrance of the phenyl ring and the methyl substituents on the pyrazole ring. Puckering analysis (Cremer & Pople, 1975) carried out in *PLATON* (Spek, 2020) showed that the methylene carbon atom (C8) on the benzodioxolyl ring (consisting of atoms O3/C4/C5/O4/C8) can be described as the flap of an envelope with a puckering amplitude Q of $0.162(2)$ Å and ψ angle of $323.1(8)^\circ$. A *Mogul* (Bruno *et al.*, 2004) geometry check as performed in *Mercury* (Macrae *et al.*, 2020) did not yield any significant unusual geometrical parameters within the structure. An intramolecular C9–H9...O2 hydrogen bond (Fig. 1, Table 1) generates an $S(6)$ ring.

Interestingly, after completing the structural refinement the structural checks suggested that the structure contains two solvent-accessible voids, each of 397 \AA^3 . The *PLATON*

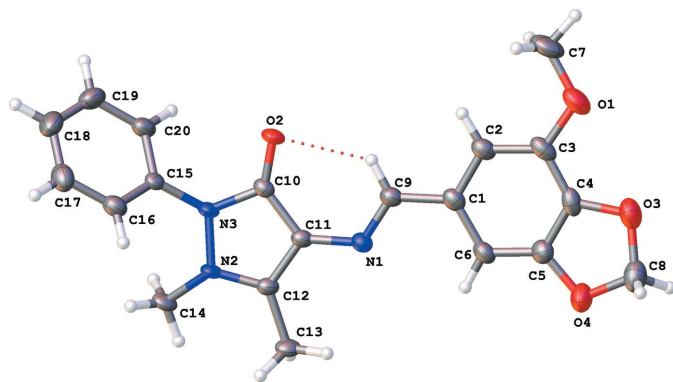


Figure 1
The molecular structure of **I**, showing the atom-labelling scheme. Displacement ellipsoids are drawn at the 50% probability level. Dashed red lines indicate hydrogen-bonding interactions.

Table 1
Hydrogen-bond geometry (Å, °).

$Cg2$ and $Cg4$ are the centroids of the pyrazole (N2/N3/C10–C12) and phenyl (C15–C20) rings, respectively.

$D-H \cdots A$	$D-H$	$H \cdots A$	$D \cdots A$	$D-H \cdots A$
C9–H9...O2	0.95	2.33	3.031 (2)	131
C13–H13A...O2 ⁱ	0.98	2.62	3.265 (2)	124
C14–H14B...O2 ⁱ	0.98	2.38	3.330 (2)	163
C20–H20...O2 ⁱⁱ	0.95	2.57	3.488 (3)	162
C14–H14C...Cg2 ⁱⁱⁱ	0.98	2.72	3.584 (3)	147
C19–H19...Cg4 ⁱⁱ	0.95	2.94	3.816 (3)	154

Symmetry codes: (i) $-x + \frac{3}{2}, y - \frac{1}{2}, -z + \frac{3}{2}$; (ii) $x, -y + 1, z + \frac{1}{2}$; (iii) $-x + \frac{3}{2}, -y + \frac{1}{2}, -z + 2$.

SQUEEZE (Spek, 2015) algorithm was applied to the refinement to explain this structural feature and assign the electron density accordingly. Since the material was synthesized in ethanol, it is likely that the voids were created by the solvent and once the crystals were extracted from the reaction mixture and the solvent evaporated, voids were formed in this way. The voids can be seen in the packing arrangement (Fig. 2).

3. Supramolecular features

Analysis of the crystal packing of **I** clearly shows the channels of void space, especially when viewed down the c -axis direction (Fig. 2). The molecules tend to stack on top of one

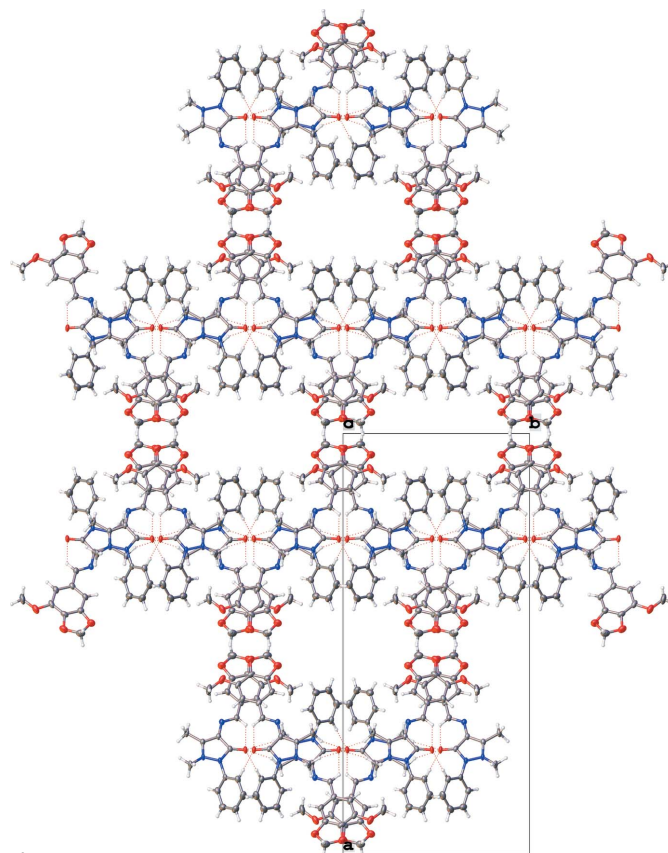


Figure 2
Packing diagram of **I** as viewed down the c -axis direction. Dashed red lines indicate hydrogen-bonding interactions.

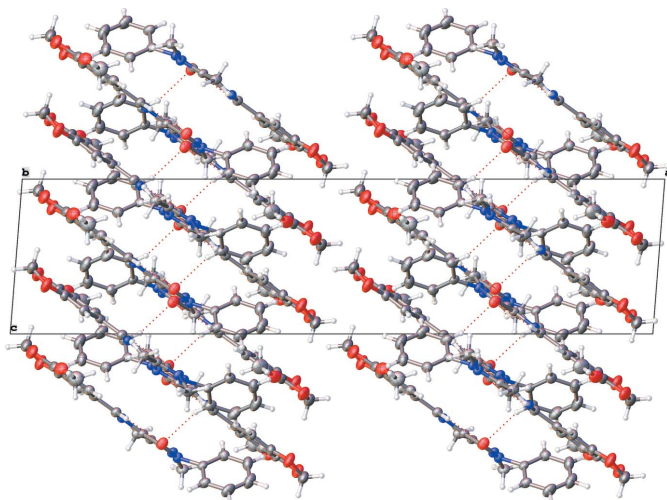


Figure 3
Packing diagram of **I** as viewed down the *b*-axis direction. Dashed red lines indicate hydrogen-bonding interactions.

another in an alternate fashion, as is evident when viewed down the *b*-axis direction (Fig. 3) with the phenyl rings protruding out of the plane every alternate layer. While there are no classical hydrogen bonds, there are hydrogen-bonding interactions present (mostly C—H···O interactions; Table 1), which help to consolidate the packing. This is particularly evident in Fig. 3 where the hydrogen bonds can be seen to be connecting layers of molecules together. The hydrogen-bonding network (three-dimensional in nature) showing the four most prominent hydrogen-bonding interactions (one being an intramolecular interaction) can be seen in Fig. 4. It may be noted that atom O2 accepts all the hydrogen bonds (one intramolecular and three intermolecular). The second graph-set that is clearly visible in Fig. 4 is a ring motif with graph-set descriptor $R_2^1(7)$. It is these intermolecular interactions that connect the molecules between layers, as shown in Fig. 3. Two weak C—H··· π interactions are also present (Table 1).

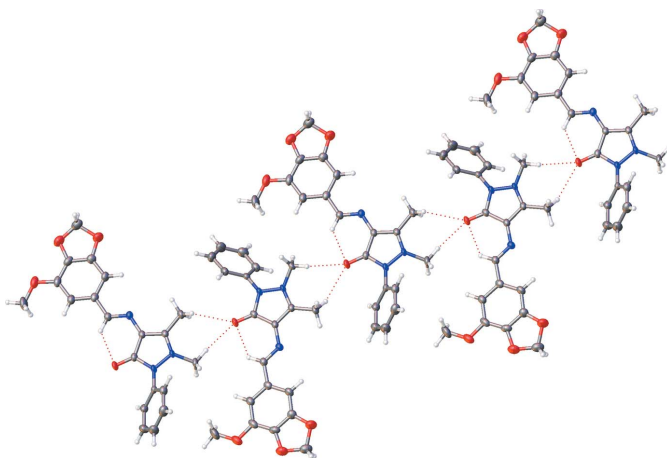


Figure 4
Detail of the structure of **I** showing three of the four hydrogen-bonding interactions; one intramolecular interaction and two of the three intermolecular interactions are indicated by dashed red lines.

4. Database survey

A search for the exact structure of the title compound in the Cambridge Structural Database (CSD Version 2020.2.0; Groom *et al.*, 2016) yielded no hits. In order to determine if the structures of other similar compounds had been published, we expanded the structure search to only include the 2,3-Dihydro-1*H*-pyrazole moiety as the backbone for other possible structures. A search was carried out in the CSD with no filters applied and this yielded 322 compounds. Of these, 92 of the compounds were coordinated to metals or were co-crystals and classified as ‘organometallic?’ under the CSD search filter. The remaining 230 compounds are then classified as ‘organic?’ under the CSD search filter. Thus, the title compound falls into this latter category.

5. Synthesis and crystallization

The title compound was prepared by reflux of a solution containing 4-amino-1,5-dimethyl-2-phenyl-1,2-dihydropyrazol-3-one (0.244 g, 1.20 mmol) in 5 ml of ethanol and a solution of 4-methoxybenzo[1,3]dioxole-5-carbaldehyde (0.179 g, 1.20 mmol) in 5 ml of ethanol. The reaction mixture was stirred for 24 h under reflux. Crystals of the title compound were obtained from ethanol solution by slow evaporation. A suitable crystal was selected from the mother liquor for the single-crystal X-ray diffraction analysis.

6. Refinement

Crystal data, data collection and structure refinement details are summarized in Table 2. The C-bound H atoms were placed in geometrically idealized positions, with C—H = 0.93–0.99 Å, and were constrained to ride on their parent atoms with relative isotropic displacement coefficients, with $U_{\text{iso}}(\text{H}) = 1.2U_{\text{eq}}(\text{C})$ for aromatic and methylene H atoms, and $U_{\text{iso}}(\text{H}) = 1.5U_{\text{eq}}(\text{C})$ for methyl H atoms. The methyl H atoms were initially located in a different-Fourier map and they were placed in idealized positions as described above and refined as rotating groups. The structure contained two solvent accessible voids of 397 Å³ each, thereby giving a total void volume of 794 Å³. No substantial electron density peaks were found in the solvent-accessible voids and the residual electron density peaks could not be arranged in an interpretable pattern. The cif and fcf files were thus corrected for using reverse Fourier transform methods using the *SQUEEZE* routine (Spek, 2015) as implemented in the program *PLATON* (Spek, 2020). The resultant files were used in the further refinement. The *SQUEEZE* procedure corrected for 28 electrons within the two solvent-accessible voids.

Acknowledgements

The Research Centre for Synthesis and Catalysis is acknowledged for providing funding for the characterization of the compounds discussed in this paper. The University of Johannesburg X-ray Diffraction Unit is acknowledged for infrastructure to collect the data of the title compound.

Funding information

Funding for this research was provided by: NRF Thuthuka Programme grant No. 117946 to C Arderne); NRF Post-doctoral Scarce Skills Fellowship scholarship No. 11670 to M. C. D. Fotsing).

References

- Bruker (2014). *APEX2*. Bruker AXS Inc., Madison, Wisconsin, USA.
- Bruker (2015). *SAINT*. Bruker AXS Inc., Madison, Wisconsin, USA.
- Bruker (2016). *SADABS*. Bruker AXS Inc., Madison, Wisconsin, USA.
- Bruno, I. J., Cole, J. C., Kessler, M., Luo, J., Motherwell, W. D. S., Purkis, L. H., Smith, B. R., Taylor, R., Cooper, R. I., Harris, S. E. & Orpen, A. G. (2004). *J. Chem. Inf. Comput. Sci.* **44**, 2133–2144.
- Cremer, D. & Pople, J. A. (1975). *J. Am. Chem. Soc.* **97**, 1354–1358.
- Deng, J., Yu, P., Zhang, Z., Zhang, J., Zhewen, S., Cai, M., Yuan, H., Liang, H. & Yang, F. (2019). *Metallomics*, **11**, 1847–1863.
- Dolomanov, O. V., Bourhis, L. J., Gildea, R. J., Howard, J. A. K. & Puschmann, H. (2009). *J. Appl. Cryst.* **42**, 339–341.
- Groom, C. R., Bruno, I. J., Lightfoot, M. P. & Ward, S. C. (2016). *Acta Cryst. B* **72**, 171–179.
- Ismail, A. H., Al-Zaidi, B. H., Abd, A. N. & Habubi, N. F. (2020). *Chem. Pap.* **74**, 2069–2078.
- Junaedi, S., Al-Amiery, A. A., Kadhum, A., Kadhum, A. A. H. & Mohamad, A. B. (2013). *Int. J. Mol. Sci.* **14**, 11915–11928.
- Keskioglu, E., Gunduzalp, A. B., Çete, S., Hamurcu, F. & Erk, B. (2008). *Spectrochim. Acta A Mol. Biomol. Spectrosc.* **70**, 634–640.
- Li, L., Wang, C., Tian, C., Yang, X., Hua, X. & Du, J. (2013). *Res. Chem. Intermed.* **39**, 733–746.
- Macrae, C. F., Sovago, I., Cottrell, S. J., Galek, P. T. A., McCabe, P., Pidcock, E., Platings, M., Shields, G. P., Stevens, J. S., Towler, M. & Wood, P. A. (2020). *J. Appl. Cryst.* **53**, 226–235.
- Murtaza, S., Akhtar, M. S., Kanwal, F., Abbas, A., Ashiq, S. & Shamim, S. (2017). *J. Saudi Chem. Soc.* **21**, S359–S372.
- Obasi, L. N., Kaior, G. U., Rhyman, L., Alswaidan, I. A., Fun, H.-K. & Ramasami, P. (2016). *J. Mol. Struct.* **1120**, 180–186.
- Rosenberg, B., Vancamp, L., Trosko, J. E. & Mansour, V. H. (1969). *Nature*, **222**, 385–386.

Table 2

Experimental details.

Crystal data	
Chemical formula	C ₂₀ H ₁₉ N ₃ O ₄
<i>M_r</i>	365.38
Crystal system, space group	Monoclinic, C2/c
Temperature (K)	173
<i>a</i> , <i>b</i> , <i>c</i> (Å)	33.888 (4), 14.9497 (18), 8.2021 (10)
β (°)	94.447 (4)
<i>V</i> (Å ³)	4142.8 (9)
<i>Z</i>	8
Radiation type	Mo <i>K</i> α
μ (mm ⁻¹)	0.08
Crystal size (mm)	0.43 × 0.37 × 0.03
Data collection	
Diffractometer	Bruker APEXII CCD
Absorption correction	Multi-scan (<i>SADABS</i> ; Bruker, 2016)
<i>T_{min}</i> , <i>T_{max}</i>	0.961, 0.969
No. of measured, independent and observed [<i>I</i> > 2 σ (<i>I</i>)] reflections	16905, 5003, 2935
<i>R_{int}</i>	0.068
(<i>sin</i> θ / λ) _{max} (Å ⁻¹)	0.660
Refinement	
<i>R</i> [<i>F</i> ² > 2 σ (<i>F</i> ²)], <i>wR</i> (<i>F</i> ²), <i>S</i>	0.063, 0.161, 1.05
No. of reflections	5003
No. of parameters	247
H-atom treatment	H-atom parameters constrained
$\Delta\rho_{\max}$, $\Delta\rho_{\min}$ (e Å ⁻³)	0.22, -0.25

Computer programs: *APEX2* (Bruker, 2014), *SAINT* (Bruker, 2015), *SHELXL2018/3* (Sheldrick, 2015), *OLEX2* (Dolomanov *et al.*, 2009).

- Sakthivel, A., Jeyasubramanian, K., Thangagiri, B. & Raja, J. D. (2020). *J. Mol. Struct.* **1222**, 128885–128900.
- Sheldrick, G. M. (2015). *Acta Cryst. C* **71**, 3–8.
- Soufeena, P. P. & Aravindakshan, K. K. (2019). *J. Lumin.* **205**, 400–405.
- Spek, A. L. (2015). *Acta Cryst. C* **71**, 9–18.
- Spek, A. L. (2020). *Acta Cryst. E* **76**, 1–11.
- Williams, A. I. (1971). *Analyst*, **96**, 296–305.

supporting information

Acta Cryst. (2021). E77, 200-203 [https://doi.org/10.1107/S2056989021000797]

Synthesis and structure of 4-[[*(E)*-(7-methoxy-1,3-benzodioxol-5-yl)methylidene]amino]-1,5-dimethyl-2-phenyl-2,3-dihydro-1*H*-pyrazol-3-one

Charmaine Arderne, Marthe Carine Djuide Fotsing and Derek Tantoh Ndinteh

Computing details

Data collection: *APEX2* (Bruker, 2014); cell refinement: *SAINTE* (Bruker, 2015); data reduction: *SAINTE* (Bruker, 2015); program(s) used to refine structure: *SHELXL2018/3* (Sheldrick, 2015); molecular graphics: *OLEX2* (Dolomanov *et al.*, 2009); software used to prepare material for publication: *OLEX2* (Dolomanov *et al.*, 2009).

4-[[*(E)*-(7-Methoxy-1,3-benzodioxol-5-yl)methylidene]amino]-1,5-dimethyl-2-phenyl-2,3-dihydro-1*H*-pyrazol-3-one

Crystal data

$C_{20}H_{19}N_3O_4$

$M_r = 365.38$

Monoclinic, *C2/c*

$a = 33.888$ (4) Å

$b = 14.9497$ (18) Å

$c = 8.2021$ (10) Å

$\beta = 94.447$ (4)°

$V = 4142.8$ (9) Å³

$Z = 8$

$F(000) = 1536$

$D_x = 1.172$ Mg m⁻³

Mo $K\alpha$ radiation, $\lambda = 0.71073$ Å

Cell parameters from 4074 reflections

$\theta = 2.9$ – 28.0 °

$\mu = 0.08$ mm⁻¹

$T = 173$ K

Plate, colourless

$0.43 \times 0.37 \times 0.03$ mm

Data collection

Bruker APEXII CCD
diffractometer

φ and ω scans

Absorption correction: multi-scan
(SADABS; Bruker, 2016)

$T_{\min} = 0.961$, $T_{\max} = 0.969$

16905 measured reflections

5003 independent reflections

2935 reflections with $I > 2\sigma(I)$

$R_{\text{int}} = 0.068$

$\theta_{\max} = 28.0$ °, $\theta_{\min} = 2.9$ °

$h = -44 \rightarrow 44$

$k = -19 \rightarrow 19$

$l = -10 \rightarrow 10$

Refinement

Refinement on F^2

Least-squares matrix: full

$R[F^2 > 2\sigma(F^2)] = 0.063$

$wR(F^2) = 0.161$

$S = 1.05$

5003 reflections

247 parameters

0 restraints

Primary atom site location: dual

Hydrogen site location: inferred from
neighbouring sites

H-atom parameters constrained

$w = 1/[\sigma^2(F_o^2) + (0.0734P)^2 + 0.941P]$

where $P = (F_o^2 + 2F_c^2)/3$

$(\Delta/\sigma)_{\max} = 0.001$

$\Delta\rho_{\max} = 0.22$ e Å⁻³

$\Delta\rho_{\min} = -0.24$ e Å⁻³

Special details

Geometry. All esds (except the esd in the dihedral angle between two l.s. planes) are estimated using the full covariance matrix. The cell esds are taken into account individually in the estimation of esds in distances, angles and torsion angles; correlations between esds in cell parameters are only used when they are defined by crystal symmetry. An approximate (isotropic) treatment of cell esds is used for estimating esds involving l.s. planes.

Fractional atomic coordinates and isotropic or equivalent isotropic displacement parameters (\AA^2)

	<i>x</i>	<i>y</i>	<i>z</i>	$U_{\text{iso}}^*/U_{\text{eq}}$
O1	0.58334 (5)	0.64735 (10)	0.2240 (2)	0.0456 (4)
O2	0.75013 (4)	0.47729 (8)	0.70830 (18)	0.0323 (4)
O3	0.53604 (5)	0.49708 (11)	0.1150 (2)	0.0494 (5)
O4	0.55059 (4)	0.34999 (10)	0.1851 (2)	0.0503 (5)
N1	0.68411 (5)	0.35046 (10)	0.54319 (19)	0.0252 (4)
N2	0.76699 (5)	0.25079 (9)	0.7655 (2)	0.0249 (4)
N3	0.77585 (5)	0.34100 (9)	0.7990 (2)	0.0255 (4)
C1	0.63820 (6)	0.45058 (13)	0.4033 (3)	0.0279 (5)
C2	0.62927 (6)	0.53913 (13)	0.3626 (3)	0.0312 (5)
H2	0.646875	0.585052	0.402084	0.037*
C3	0.59537 (7)	0.56216 (13)	0.2659 (3)	0.0340 (5)
C4	0.57152 (6)	0.49285 (15)	0.2094 (3)	0.0340 (5)
C5	0.58021 (6)	0.40553 (14)	0.2506 (3)	0.0327 (5)
C6	0.61272 (6)	0.38165 (14)	0.3489 (3)	0.0312 (5)
H6	0.617801	0.321120	0.378844	0.037*
C7	0.60737 (8)	0.71811 (15)	0.2899 (4)	0.0576 (8)
H7A	0.595674	0.775502	0.254306	0.086*
H7B	0.633927	0.712931	0.251285	0.086*
H7C	0.609129	0.714853	0.409539	0.086*
C8	0.52643 (7)	0.40623 (16)	0.0732 (3)	0.0467 (6)
H8A	0.532170	0.393770	-0.041099	0.056*
H8B	0.497994	0.394756	0.084311	0.056*
C9	0.67425 (6)	0.43094 (12)	0.5059 (2)	0.0277 (5)
H9	0.690725	0.478813	0.545809	0.033*
C10	0.74742 (5)	0.39514 (12)	0.7154 (2)	0.0238 (4)
C11	0.71847 (6)	0.33316 (12)	0.6432 (2)	0.0237 (4)
C12	0.73153 (6)	0.24798 (12)	0.6818 (2)	0.0243 (4)
C13	0.71041 (6)	0.16214 (12)	0.6430 (3)	0.0306 (5)
H13A	0.729441	0.116956	0.612385	0.046*
H13B	0.690370	0.171445	0.551884	0.046*
H13C	0.697547	0.141629	0.739228	0.046*
C14	0.78468 (6)	0.18201 (12)	0.8739 (3)	0.0299 (5)
H14A	0.811992	0.171173	0.847614	0.045*
H14B	0.769373	0.126576	0.859300	0.045*
H14C	0.784562	0.202030	0.987620	0.045*
C15	0.81520 (6)	0.36838 (12)	0.8489 (2)	0.0239 (4)
C16	0.84730 (6)	0.32824 (13)	0.7854 (3)	0.0328 (5)
H16	0.843312	0.281952	0.706444	0.039*
C17	0.88527 (7)	0.35536 (15)	0.8364 (3)	0.0430 (6)

H17	0.907443	0.327095	0.794364	0.052*
C18	0.89074 (7)	0.42389 (15)	0.9491 (3)	0.0501 (7)
H18	0.916768	0.442702	0.984695	0.060*
C19	0.85839 (7)	0.46524 (15)	1.0102 (3)	0.0470 (6)
H19	0.862273	0.513220	1.085733	0.056*
C20	0.82043 (7)	0.43677 (13)	0.9616 (3)	0.0328 (5)
H20	0.798210	0.464009	1.005186	0.039*

Atomic displacement parameters (Å²)

	U^{11}	U^{22}	U^{33}	U^{12}	U^{13}	U^{23}
O1	0.0564 (11)	0.0334 (9)	0.0463 (10)	0.0173 (8)	-0.0007 (8)	0.0064 (7)
O2	0.0376 (9)	0.0122 (7)	0.0458 (10)	0.0028 (6)	-0.0055 (7)	-0.0010 (6)
O3	0.0397 (10)	0.0505 (11)	0.0560 (12)	0.0124 (8)	-0.0105 (8)	0.0039 (8)
O4	0.0374 (9)	0.0456 (10)	0.0646 (12)	0.0024 (8)	-0.0170 (8)	0.0046 (8)
N1	0.0277 (9)	0.0207 (8)	0.0271 (10)	0.0021 (7)	0.0011 (7)	0.0018 (7)
N2	0.0330 (10)	0.0104 (8)	0.0303 (10)	0.0012 (7)	-0.0037 (7)	0.0008 (7)
N3	0.0304 (9)	0.0126 (8)	0.0327 (10)	0.0015 (7)	-0.0023 (7)	-0.0003 (7)
C1	0.0322 (11)	0.0269 (11)	0.0250 (11)	0.0068 (9)	0.0044 (9)	-0.0002 (8)
C2	0.0389 (12)	0.0241 (11)	0.0305 (12)	0.0062 (9)	0.0019 (10)	0.0004 (9)
C3	0.0440 (13)	0.0270 (11)	0.0316 (13)	0.0136 (10)	0.0072 (10)	0.0051 (9)
C4	0.0290 (12)	0.0429 (13)	0.0297 (13)	0.0119 (10)	-0.0009 (10)	0.0036 (10)
C5	0.0275 (11)	0.0328 (12)	0.0378 (13)	0.0024 (9)	0.0024 (10)	-0.0017 (10)
C6	0.0323 (12)	0.0248 (11)	0.0361 (13)	0.0085 (9)	0.0011 (10)	0.0012 (9)
C7	0.0775 (19)	0.0230 (12)	0.072 (2)	0.0129 (13)	0.0009 (16)	0.0026 (12)
C8	0.0350 (13)	0.0563 (16)	0.0472 (16)	0.0013 (12)	-0.0059 (11)	0.0091 (12)
C9	0.0320 (11)	0.0213 (10)	0.0295 (12)	0.0017 (8)	0.0000 (9)	-0.0006 (8)
C10	0.0273 (11)	0.0189 (10)	0.0253 (11)	0.0041 (8)	0.0027 (8)	0.0016 (8)
C11	0.0307 (11)	0.0173 (9)	0.0228 (11)	0.0004 (8)	0.0005 (9)	-0.0004 (8)
C12	0.0316 (11)	0.0177 (9)	0.0231 (11)	-0.0008 (8)	-0.0002 (9)	-0.0007 (8)
C13	0.0417 (12)	0.0166 (9)	0.0328 (12)	-0.0037 (9)	-0.0011 (10)	0.0030 (8)
C14	0.0438 (13)	0.0146 (9)	0.0306 (12)	0.0041 (9)	-0.0022 (10)	0.0051 (8)
C15	0.0288 (11)	0.0153 (9)	0.0265 (11)	0.0022 (8)	-0.0044 (9)	0.0034 (8)
C16	0.0379 (13)	0.0243 (10)	0.0359 (13)	0.0049 (9)	0.0008 (10)	0.0001 (9)
C17	0.0308 (12)	0.0394 (13)	0.0582 (17)	0.0023 (10)	0.0003 (11)	0.0085 (12)
C18	0.0396 (14)	0.0363 (13)	0.0710 (19)	-0.0072 (11)	-0.0175 (13)	0.0039 (13)
C19	0.0533 (16)	0.0303 (12)	0.0539 (17)	-0.0060 (11)	-0.0179 (13)	-0.0055 (11)
C20	0.0421 (13)	0.0218 (10)	0.0332 (13)	0.0053 (9)	-0.0055 (10)	-0.0020 (9)

Geometric parameters (Å, °)

O1—C3	1.373 (2)	C7—H7C	0.9800
O1—C7	1.416 (3)	C8—H8A	0.9900
O2—C10	1.233 (2)	C8—H8B	0.9900
O3—C4	1.380 (3)	C9—H9	0.9500
O3—C8	1.432 (3)	C10—C11	1.443 (3)
O4—C5	1.379 (2)	C11—C12	1.377 (2)
O4—C8	1.450 (3)	C12—C13	1.492 (3)

N1—C9	1.279 (2)	C13—H13A	0.9800
N1—C11	1.396 (2)	C13—H13B	0.9800
N2—N3	1.404 (2)	C13—H13C	0.9800
N2—C12	1.337 (2)	C14—H14A	0.9800
N2—C14	1.458 (2)	C14—H14B	0.9800
N3—C10	1.397 (2)	C14—H14C	0.9800
N3—C15	1.424 (2)	C15—C16	1.379 (3)
C1—C2	1.393 (3)	C15—C20	1.380 (3)
C1—C6	1.395 (3)	C16—H16	0.9500
C1—C9	1.459 (3)	C16—C17	1.383 (3)
C2—H2	0.9500	C17—H17	0.9500
C2—C3	1.388 (3)	C17—C18	1.382 (3)
C3—C4	1.372 (3)	C18—H18	0.9500
C4—C5	1.374 (3)	C18—C19	1.386 (3)
C5—C6	1.361 (3)	C19—H19	0.9500
C6—H6	0.9500	C19—C20	1.384 (3)
C7—H7A	0.9800	C20—H20	0.9500
C7—H7B	0.9800		
C3—O1—C7	116.55 (18)	N1—C9—H9	119.4
C4—O3—C8	105.24 (17)	C1—C9—H9	119.4
C5—O4—C8	104.81 (16)	O2—C10—N3	123.30 (17)
C9—N1—C11	120.35 (17)	O2—C10—C11	132.15 (17)
N3—N2—C14	119.11 (15)	N3—C10—C11	104.50 (15)
C12—N2—N3	107.50 (14)	N1—C11—C10	129.19 (16)
C12—N2—C14	126.98 (16)	C12—C11—N1	123.04 (17)
N2—N3—C15	120.91 (15)	C12—C11—C10	107.67 (17)
C10—N3—N2	109.35 (15)	N2—C12—C11	110.41 (16)
C10—N3—C15	124.72 (15)	N2—C12—C13	122.25 (17)
C2—C1—C6	120.48 (19)	C11—C12—C13	127.32 (18)
C2—C1—C9	119.11 (19)	C12—C13—H13A	109.5
C6—C1—C9	120.40 (18)	C12—C13—H13B	109.5
C1—C2—H2	119.1	C12—C13—H13C	109.5
C3—C2—C1	121.9 (2)	H13A—C13—H13B	109.5
C3—C2—H2	119.1	H13A—C13—H13C	109.5
O1—C3—C2	126.1 (2)	H13B—C13—H13C	109.5
C4—C3—O1	117.4 (2)	N2—C14—H14A	109.5
C4—C3—C2	116.44 (19)	N2—C14—H14B	109.5
C3—C4—O3	128.3 (2)	N2—C14—H14C	109.5
C3—C4—C5	121.7 (2)	H14A—C14—H14B	109.5
C5—C4—O3	110.0 (2)	H14A—C14—H14C	109.5
C4—C5—O4	109.91 (18)	H14B—C14—H14C	109.5
C6—C5—O4	127.15 (19)	C16—C15—N3	120.95 (17)
C6—C5—C4	122.9 (2)	C16—C15—C20	120.75 (19)
C1—C6—H6	121.7	C20—C15—N3	118.30 (18)
C5—C6—C1	116.63 (19)	C15—C16—H16	120.0
C5—C6—H6	121.7	C15—C16—C17	120.0 (2)
O1—C7—H7A	109.5	C17—C16—H16	120.0

O1—C7—H7B	109.5	C16—C17—H17	120.2
O1—C7—H7C	109.5	C18—C17—C16	119.6 (2)
H7A—C7—H7B	109.5	C18—C17—H17	120.2
H7A—C7—H7C	109.5	C17—C18—H18	119.9
H7B—C7—H7C	109.5	C17—C18—C19	120.2 (2)
O3—C8—O4	106.97 (18)	C19—C18—H18	119.9
O3—C8—H8A	110.3	C18—C19—H19	119.9
O3—C8—H8B	110.3	C20—C19—C18	120.1 (2)
O4—C8—H8A	110.3	C20—C19—H19	119.9
O4—C8—H8B	110.3	C15—C20—C19	119.3 (2)
H8A—C8—H8B	108.6	C15—C20—H20	120.4
N1—C9—C1	121.24 (18)	C19—C20—H20	120.4
O1—C3—C4—O3	-0.6 (3)	C6—C1—C9—N1	2.6 (3)
O1—C3—C4—C5	-177.19 (19)	C7—O1—C3—C2	-1.8 (3)
O2—C10—C11—N1	-0.8 (4)	C7—O1—C3—C4	177.1 (2)
O2—C10—C11—C12	175.6 (2)	C8—O3—C4—C3	172.5 (2)
O3—C4—C5—O4	-0.3 (2)	C8—O3—C4—C5	-10.5 (2)
O3—C4—C5—C6	-177.30 (19)	C8—O4—C5—C4	10.8 (2)
O4—C5—C6—C1	-178.5 (2)	C8—O4—C5—C6	-172.3 (2)
N1—C11—C12—N2	173.82 (17)	C9—N1—C11—C10	-1.2 (3)
N1—C11—C12—C13	-7.4 (3)	C9—N1—C11—C12	-177.11 (18)
N2—N3—C10—O2	-171.96 (17)	C9—C1—C2—C3	-179.79 (19)
N2—N3—C10—C11	5.89 (19)	C9—C1—C6—C5	-178.54 (19)
N2—N3—C15—C16	36.3 (3)	C10—N3—C15—C16	-115.9 (2)
N2—N3—C15—C20	-144.29 (18)	C10—N3—C15—C20	63.5 (3)
N3—N2—C12—C11	6.5 (2)	C10—C11—C12—N2	-2.8 (2)
N3—N2—C12—C13	-172.36 (16)	C10—C11—C12—C13	175.95 (18)
N3—C10—C11—N1	-178.37 (18)	C11—N1—C9—C1	-179.18 (17)
N3—C10—C11—C12	-2.0 (2)	C12—N2—N3—C10	-7.8 (2)
N3—C15—C16—C17	-179.51 (18)	C12—N2—N3—C15	-163.85 (17)
N3—C15—C20—C19	-179.17 (19)	C14—N2—N3—C10	-161.64 (16)
C1—C2—C3—O1	177.54 (19)	C14—N2—N3—C15	42.3 (2)
C1—C2—C3—C4	-1.4 (3)	C14—N2—C12—C11	157.66 (18)
C2—C1—C6—C5	2.4 (3)	C14—N2—C12—C13	-21.2 (3)
C2—C1—C9—N1	-178.33 (19)	C15—N3—C10—O2	-17.0 (3)
C2—C3—C4—O3	178.5 (2)	C15—N3—C10—C11	160.81 (18)
C2—C3—C4—C5	1.9 (3)	C15—C16—C17—C18	-1.2 (3)
C3—C4—C5—O4	176.88 (19)	C16—C15—C20—C19	0.2 (3)
C3—C4—C5—C6	-0.1 (3)	C16—C17—C18—C19	-0.1 (4)
C4—O3—C8—O4	16.9 (2)	C17—C18—C19—C20	1.4 (4)
C4—C5—C6—C1	-2.1 (3)	C18—C19—C20—C15	-1.5 (3)
C5—O4—C8—O3	-17.1 (2)	C20—C15—C16—C17	1.1 (3)
C6—C1—C2—C3	-0.8 (3)		

Hydrogen-bond geometry (Å, °)

*Cg*2 and *Cg*4 are the centroids of the pyrazole (N2/N3/C10–C12) and phenyl (C15–C20) rings, respectively.

<i>D</i> —H··· <i>A</i>	<i>D</i> —H	H··· <i>A</i>	<i>D</i> ··· <i>A</i>	<i>D</i> —H··· <i>A</i>
C9—H9···O2	0.95	2.33	3.031 (2)	131
C13—H13 <i>A</i> ···O2 ⁱ	0.98	2.62	3.265 (2)	124
C14—H14 <i>B</i> ···O2 ⁱ	0.98	2.38	3.330 (2)	163
C20—H20···O2 ⁱⁱ	0.95	2.57	3.488 (3)	162
C14—H14 <i>C</i> ··· <i>Cg</i> 2 ⁱⁱⁱ	0.98	2.72	3.584 (3)	147
C19—H19··· <i>Cg</i> 4 ⁱⁱ	0.95	2.94	3.816 (3)	154

Symmetry codes: (i) $-x+3/2, y-1/2, -z+3/2$; (ii) $x, -y+1, z+1/2$; (iii) $-x+3/2, -y+1/2, -z+2$.